Modelling and Simulating Particle Transport in Liquid Composite Moulding Processes

The 17th International Conference on Flow Processes in Composite Materials (FPCM17)

30th June – 2nd July 2026, The University of Sheffield, UK

Shanthar Rajinth

rajinth.shanthar@manchester.ac.uk

Supervised by

Dr. Robert Prosser[1], Dr. Pavel Simacek[2], Prof. Prasad Potluri[1], Dr. Chamil Abeykoon[1], Prof. Suresh G. Advani[2]

[1]Department of Materials, The University of Manchester, United Kingdom; [2]Center for Composite Materials, University of Delaware, USA

Content

1. Introduction
- 1.1. RTM Process Overview
- 1.2. Particle Mixed Resin Flow

2. Methodology
- 2.2. Governing Equations for Particle Transport
- 2.3. Liquid Injection Molding Simulation (LIMS) Software
- 2.4. Message Passing Interface (MPI)
- 2.5. LIMS-MPI
- 2.6. Particles and Viscosity
- 2.7. Particles and Permeability
- 2.8. Transport Model Configuration

3. Results
- 3.1. Numerical Flow Domain
- 3.2. Partially Coupled Model
- 3.3. Fully Coupled Model
- 3.4. Impact of Particle Presence
- 3.5. Mould Fill Time under Fixed Pressure Injection
- 3.6. Pressure at Inlet under Fixed Flowrate Injection
- 3.7. Influence of Filtration Coefficient
- 3.8. Influence of Racetracking

4. Summary and Outlook

1. Introduction

1.1. RTM Process Overview

- Resin Transfer Moulding (RTM) is a process used to manufacture Fibre Reinforced Polymers (FRP), which consists of 5 steps as shown in Fig. 1 [1].

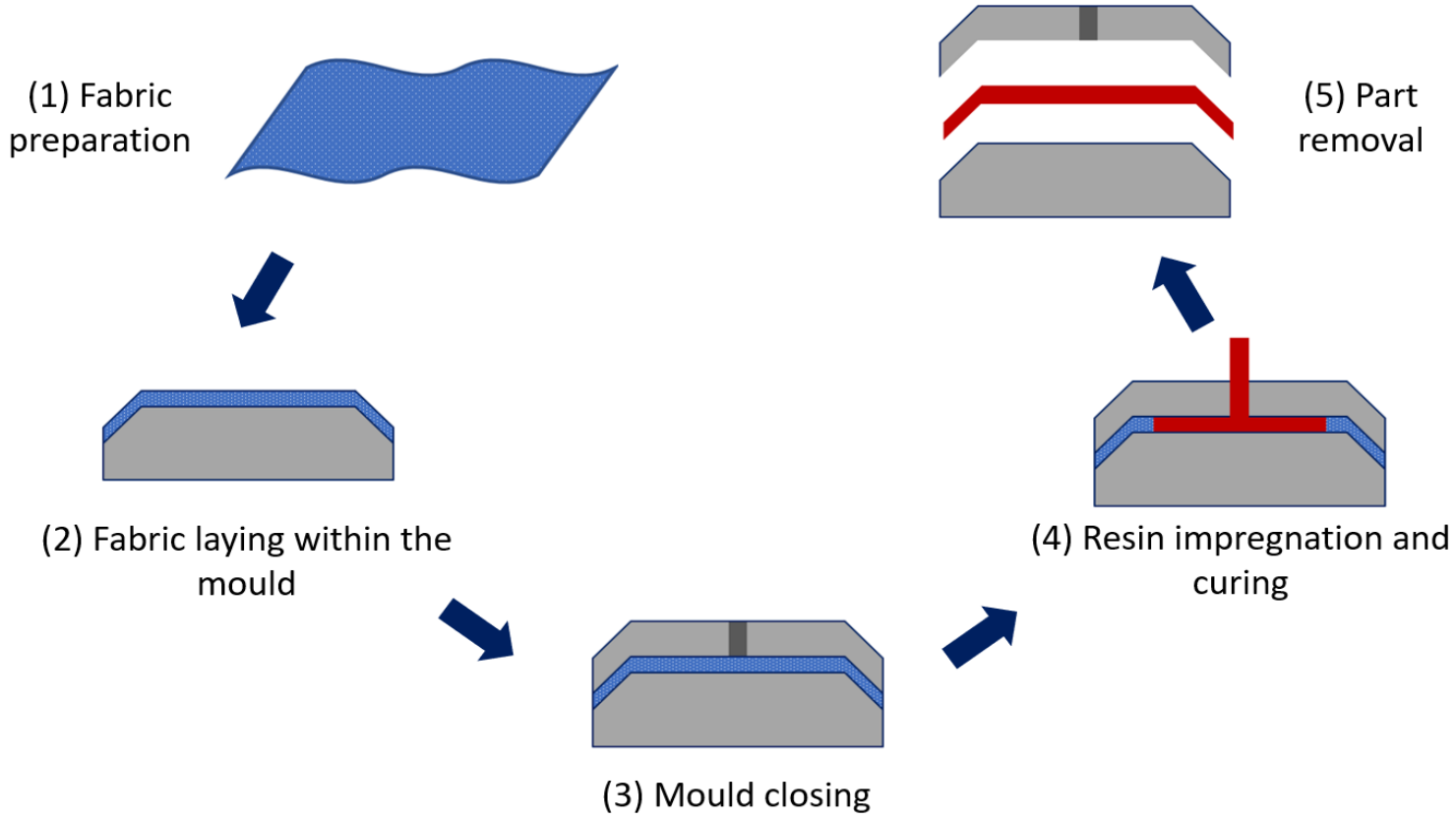

Figure 1: The Resin Transfer Moulding (RTM) process

1. Introduction

1.2. Particle Mixed Resin Flow

- Particles may be mixed with the resin to improve the properties of parts manufactured using RTM [2][3].
- The sizes of these particles can range from the micrometre scale to the nanometre scale, as shown in Fig. 2.
- The presence of particles within the resin affects the resin viscosity, and filtered particles affect the permeability of the flow channels
- Both of these phenomena subsequently affect the flow of particles during infusion [4][5].
- Transport models and simulations can provide valuable information regarding particle filtration and the final particle distribution [6].

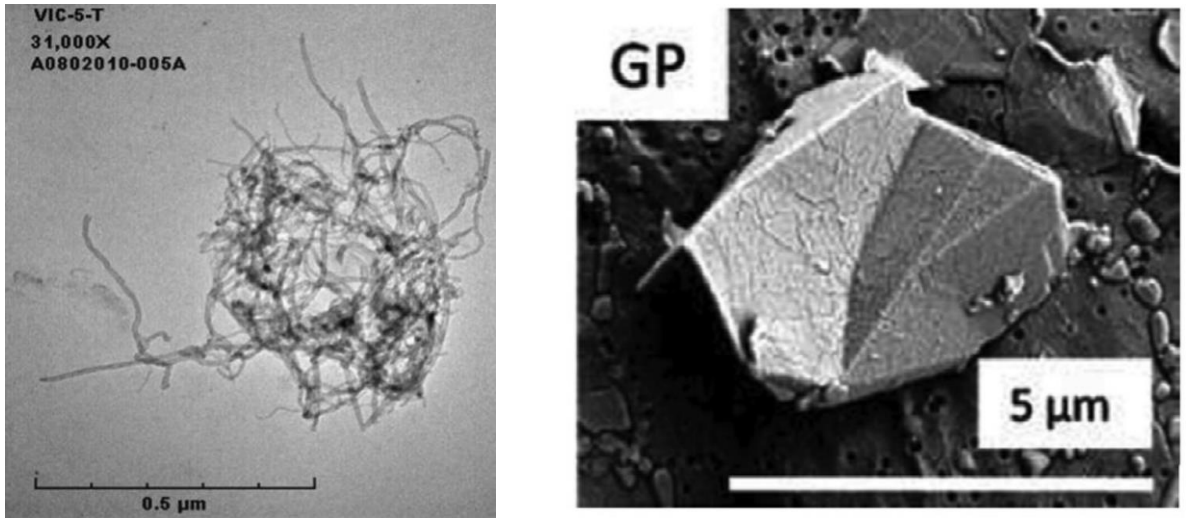

Figure 2: Different types of particles (a) Multi-Walled Carbon Nanotubes (b) Graphene Nanoplatelets [6]

2. Methodology

2.1. Governing Equations for Resin Flow

- The resin flow through the reinforcement preform is modelled as a flow through a porous medium, governed by the mass conservation equation (Eq. 1) and the Darcy equation (Eq. 2).

$$\boldsymbol{\nabla} \cdot \mathbf{u} = 0 \tag{1}$$

$$\mathbf{u} = -\frac{\mathbf{K}}{\mu}\nabla P \tag{2}$$

- Here, $\mathbf{u}$ is the volume-averaged resin velocity, $\mathbf{K}$ is the permeability tensor for the porous preform, μ is the resin viscosity, and P is the resin pressure.

- The above equations can be combined to obtain Eq. 3, which is then used to solve for the in-mould pressure distribution at each time step.

$$\boldsymbol{\nabla} \cdot \left(\frac{\mathbf{K}}{\mu}\nabla P\right) = 0 \tag{3}$$

2. Methodology

2.2. Governing Equations for Particle Transport

- Eulerian descriptions are suitable for modelling the transport of fine particles, where the number of individual particles can be extremely large.
- It has been observed experimentally that particles tend to get filtered as the resin impregnates the reinforcement (Fig. 3).
- These dynamics can be modelled by introducing appropriate sink/ source terms in transport equations [7].

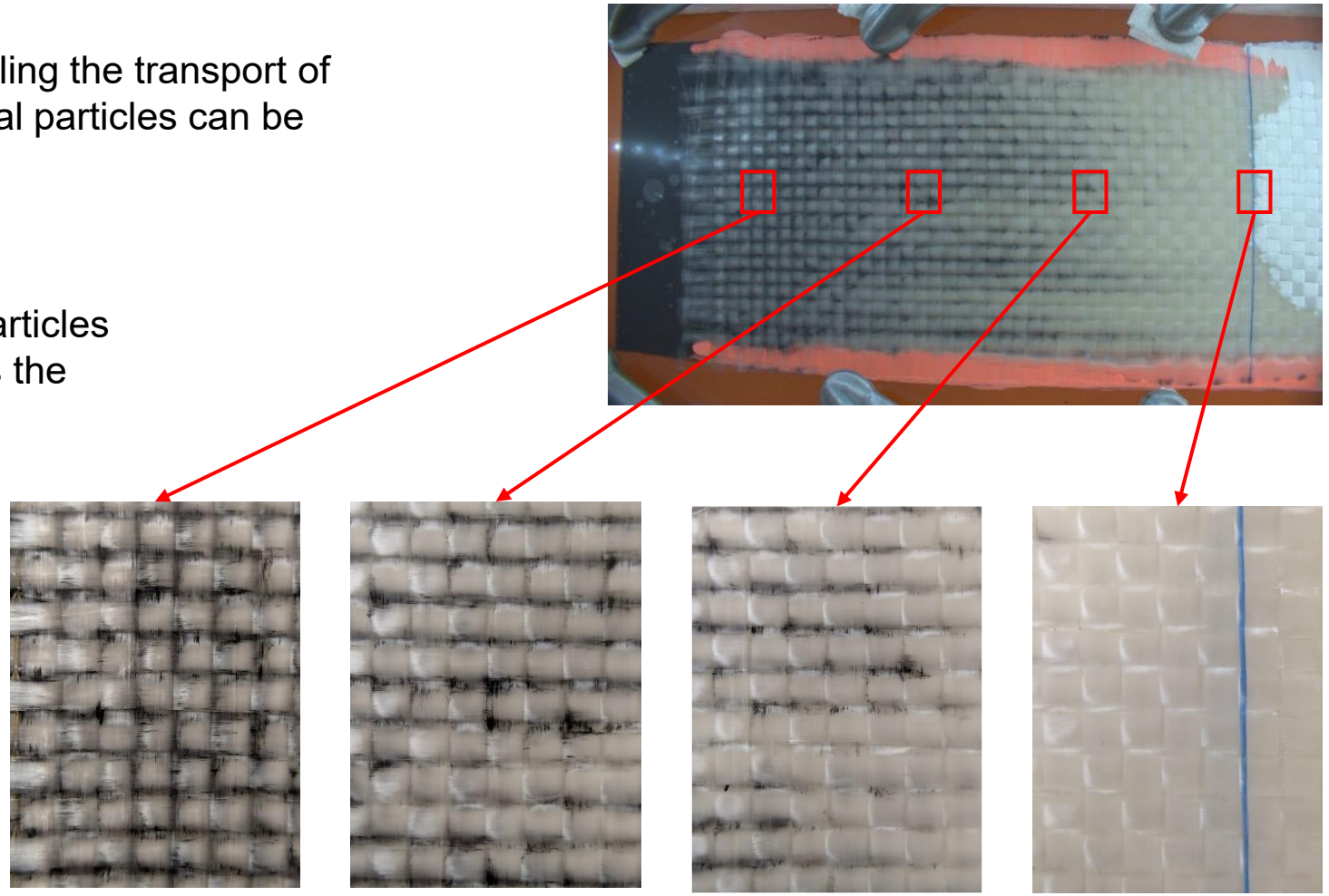

Figure 3: Filtration of GNP through the reinforcement, resulting in a non-uniform distribution of nanofillers.

2. Methodology

2.2. Governing Equations for Particle Transport

- These dynamics can be modelled by introducing appropriate sink/ source terms in the transport equations (Eqs. 4 and 5) [7][8].

$$\frac{\partial \phi C_1}{\partial t} + \nabla \cdot (\mathbf{u} C_1) = -S_{filtered} \qquad (4)$$

$$\frac{\partial C_2}{\partial t} = +S_{filtered} \qquad (5)$$

C_1 = Mass concentration of particles in the **resin** (kg/m^3_{fluid})

C_2 = Mass concentration of **filtered** particles (kg/m^3_{total})

(= Mass concentration of filtered particles)

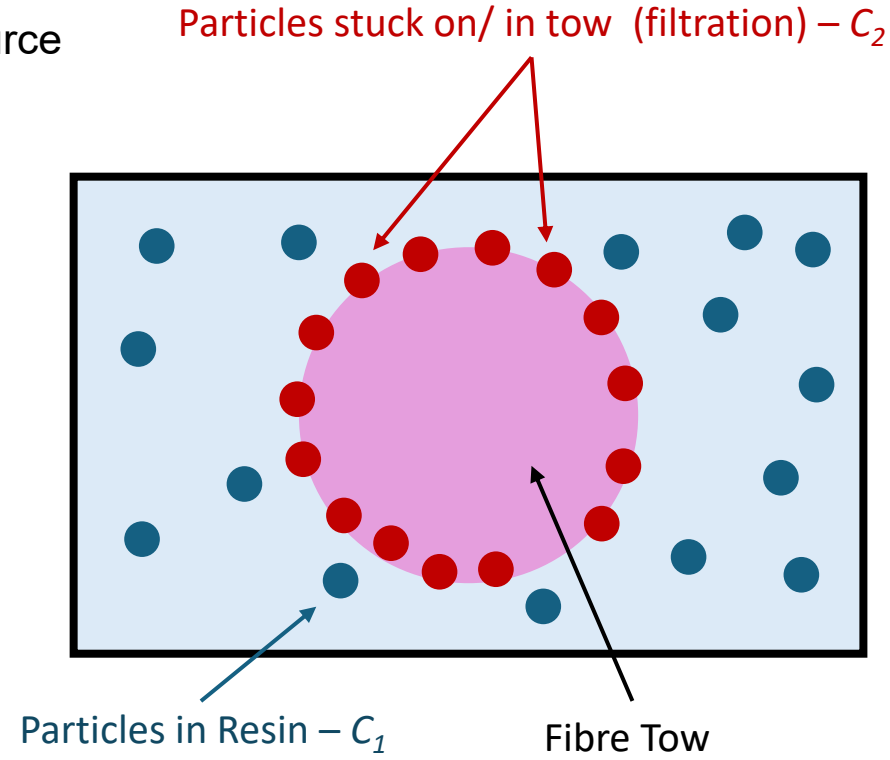

Figure 4: Classification of different particle species

2. Methodology

2.2. Governing Equations for Particle Transport

- These dynamics can be modelled by introducing appropriate sink/ source terms in the transport equations (Eqs. 4 and 5) [7][8].

$$\frac{\partial \phi C_1}{\partial t} + \nabla \cdot (\mathbf{u} C_1) = -S_{filtered} \qquad (4)$$

$$\frac{\partial C_2}{\partial t} = +S_{filtered} \qquad (5)$$

C_1 = Mass concentration of particles in the **resin** (kg/m^3_{fluid})

C_2 = Mass concentration of **filtered** particles (kg/m^3_{total})

(= Mass concentration of filtered particles)

$$S_{filtered} = k\mathbf{u}C_1 \qquad (6)$$

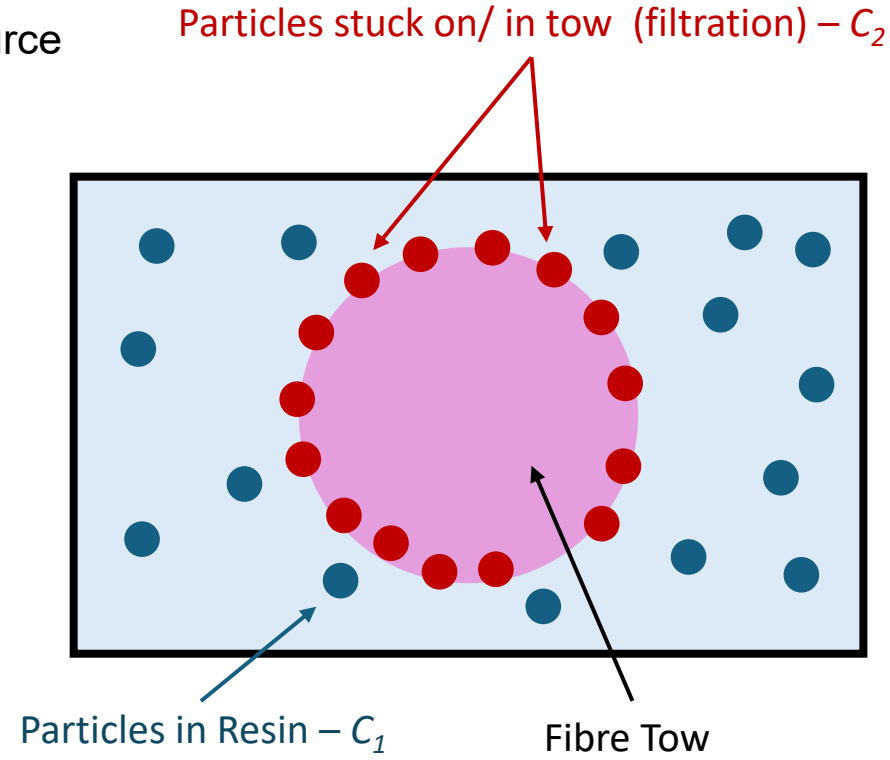

Figure 4: Classification of different particle species

- $S_{filtered}$ is the rate of particle filtration, and can be expressed using Eq. 6. Here, k is the **filtration coefficient** [8][9].

2. Methodology

2.2. Governing Equations for Particle Transport

- These dynamics can be modelled by introducing appropriate sink/ source terms in the transport equations (Eqs. 4 and 5) [7][8].

$$\frac{\partial \phi C_1}{\partial t} + \nabla \cdot (\mathbf{u} C_1) = -S_{filtered} \quad (4)$$

C_1 = Mass concentration of particles in the resin

$$\frac{\partial C_2}{\partial t} = +S_{filtered} \quad (5)$$

C_2 = Mass concentration of filtered particles

$$S_{filtered} = k\mathbf{u}C_1 \quad (6)$$

- Furthermore, it has also been observed that the reinforcement permeability and the resin viscosity are influenced by the presence of particles [10][11].

- This can be conveniently implemented in LIMS-MPI.

$$\nabla \cdot \left(\frac{\mathbf{K}}{\mu} \nabla P \right) = 0$$

$\mathbf{K}(C_2)$

$\mu(C_1)$

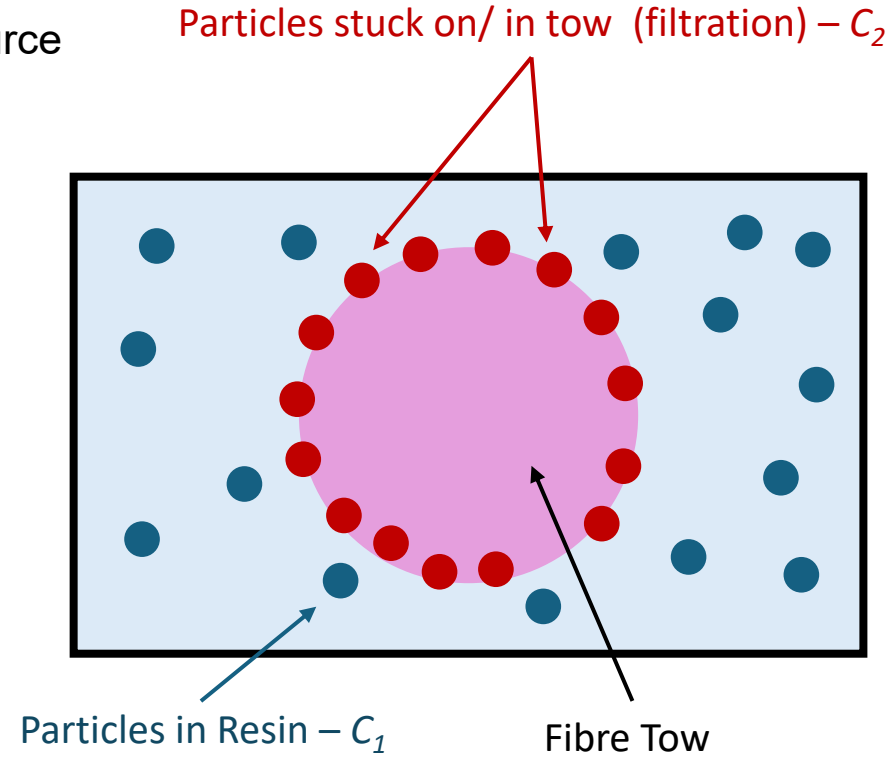

Figure 4: Classification of different particle species

2. Methodology

2.3. Liquid Injection Molding Simulation (LIMS) Software

- Research software developed at the Center for Composite Materials, University of Delaware.
- Simulates the mold-filling stage of liquid composite molding processes.
- Predicts resin flow, pressure distribution, fill time, and flow-front progression. Also supports process design for injection and venting strategies (Fig. 5).

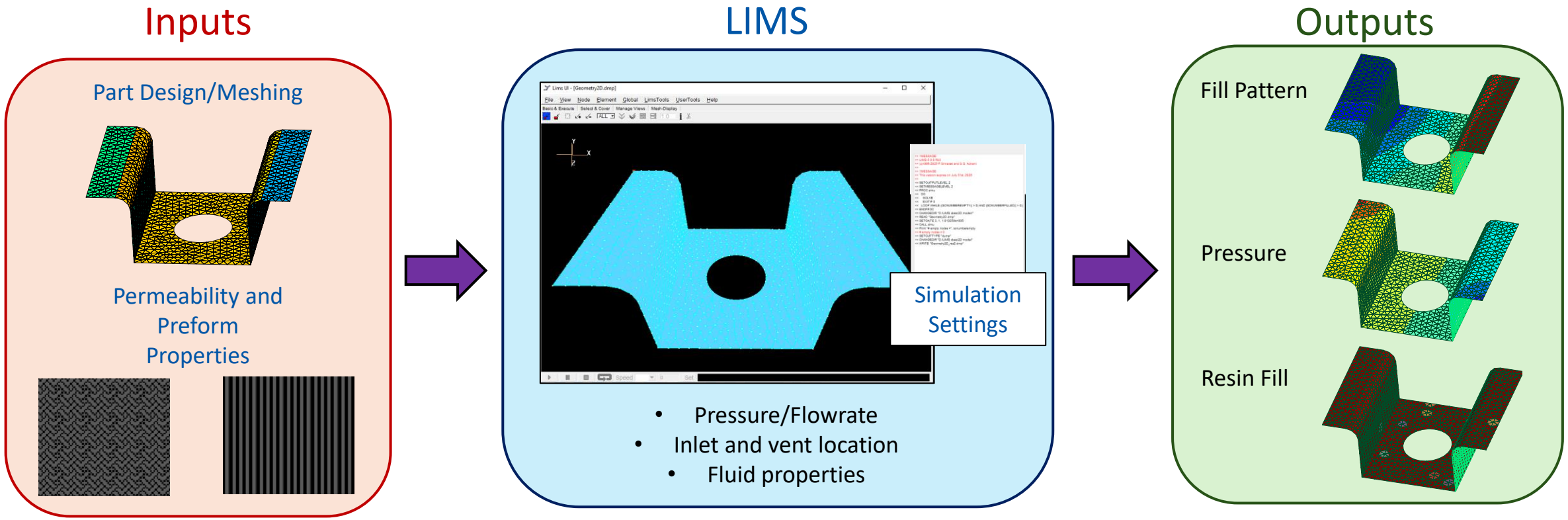

Figure 5: LIMS Software Overview

2. Methodology

2.3. Liquid Injection Molding Simulation (LIMS) Software

- LIMS simulation example:
  Automotive B-pillar (Fig. 6)

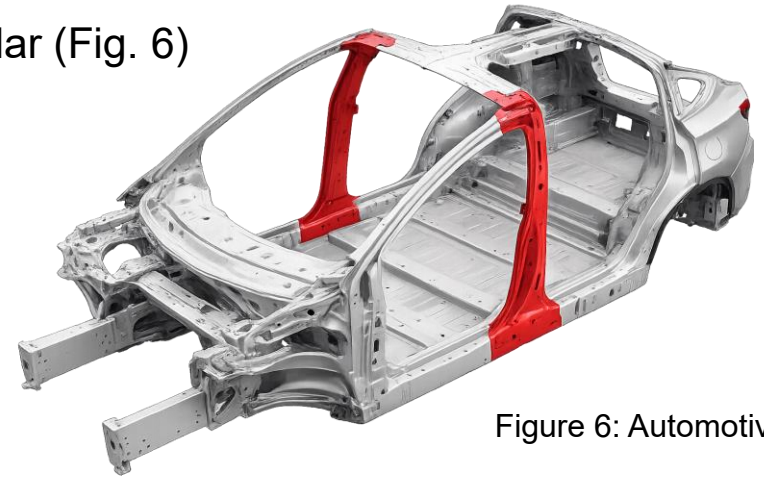

Figure 6: Automotive B-pillar

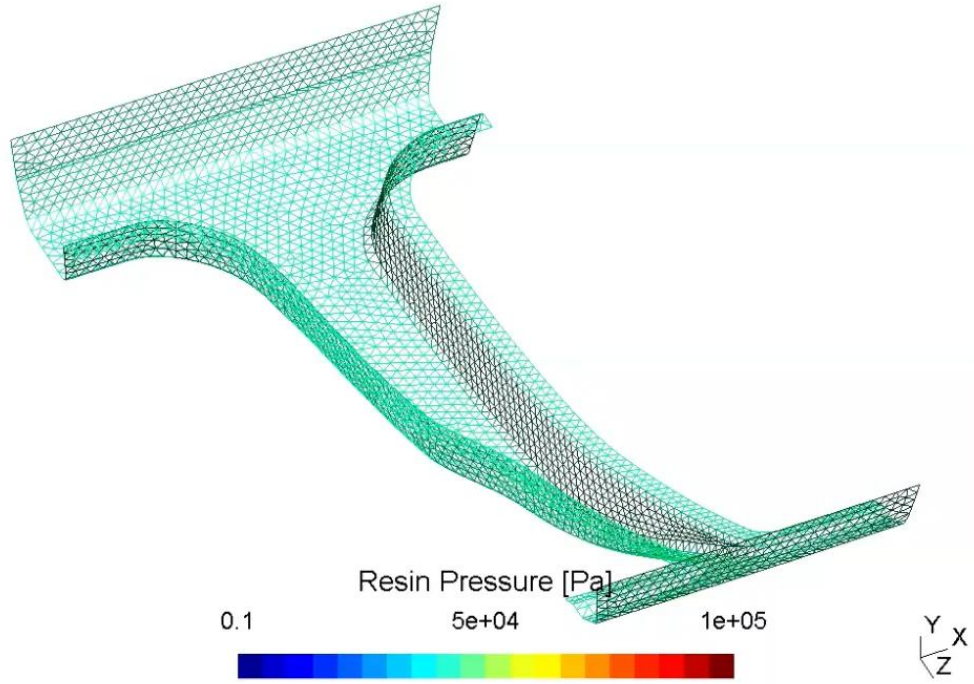

- Previously shown by LIMS:
  - ✓ Flow through porous media,
  - ✓ Deformation of flow domain,
  - ✓ Energy transport and cure evolution.

- What had not been addressed:
  - × Volatile transport and accumulation
    - Discrete entities (bubbles)
    - Dissolved volatiles
  - × Multiple species reaction
  - × **Particle transport**

Challenge: Model coupling directly into code is difficult

Approach: Develop parallel decoupled models

2. Methodology

2.4. Message Passing Interface (MPI)

- MPI is the standard framework for parallel computing and allows separate simulation codes to exchange data during runtime.
- Useful when one model controls flow while another solves additional physics.

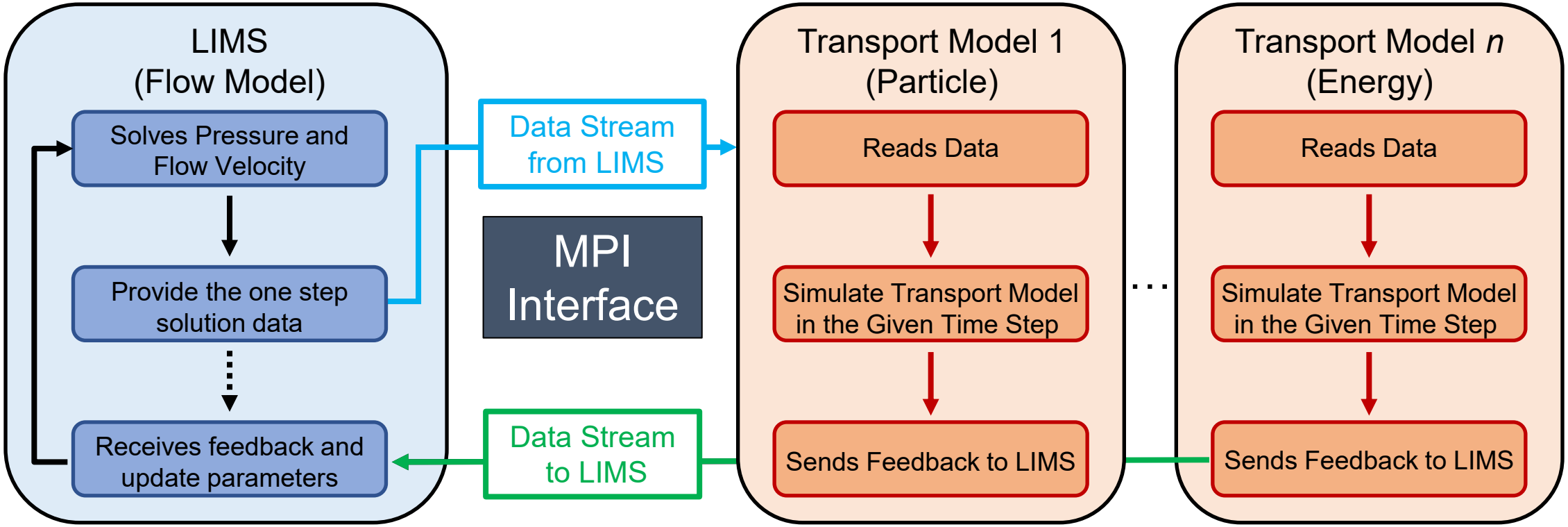

Figure 7: MPI Operation

- ✓ Multiple models run in parallel, while LIMS remains as the main flow solver.
- ✓ Data transfer occurs only at LIMS timesteps.
- ✓ MPI enables execution across multiple cores / CPUs.

2. Methodology

2.5. LIMS-MPI

- Transport Modeling Description
  - ✓ Kinematic equation for particle motion.
  - ✓ Particle concentration transport with source/sink terms
  - ✓ Modified Gebart equation for permeability variation
  - ✓ Modified Kriegher-Dougherty equation for viscosity variation
- Necessary Model Parameters
  - ✓ Filtration coefficient
  - ✓ Viscosity coefficient

- ***LIMS*** harnesses "Transport Code" functionality through the internal LBASIC script.

- ***Transport Model 1*** provides the "Common" simulation functionality and communication.

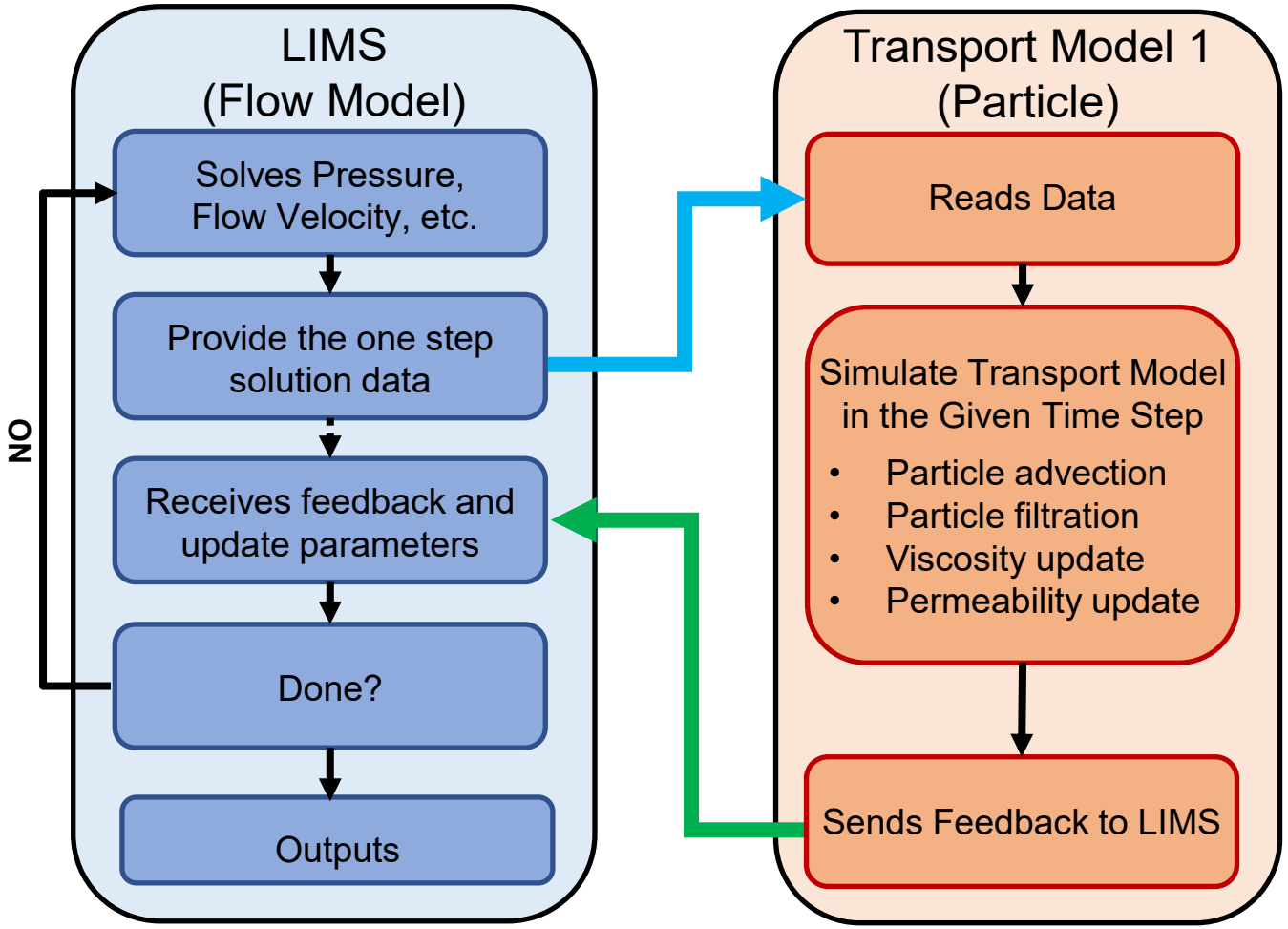

Figure 8: LIMS-MPI Overview [12]

2. Methodology

2.6. Particles and Viscosity

- The presence of particles changes the viscosity of the resin, thus, it is a function of the particle concentration within the resin.

$$\mu = \mu_0 \left(1 - \frac{C_1}{A}\right)^{-2} \qquad (8)$$

- The viscosity variation can be modelled using Eq. 8. Here, μ_0 is pure resin viscosity, and A is a constant [8][13].

- This relation is valid for non-interacting particles with a narrow size distribution [7].

- As illustrated in Fig. 10, the resin viscosity and its rate of variation increase with the particle concentration.

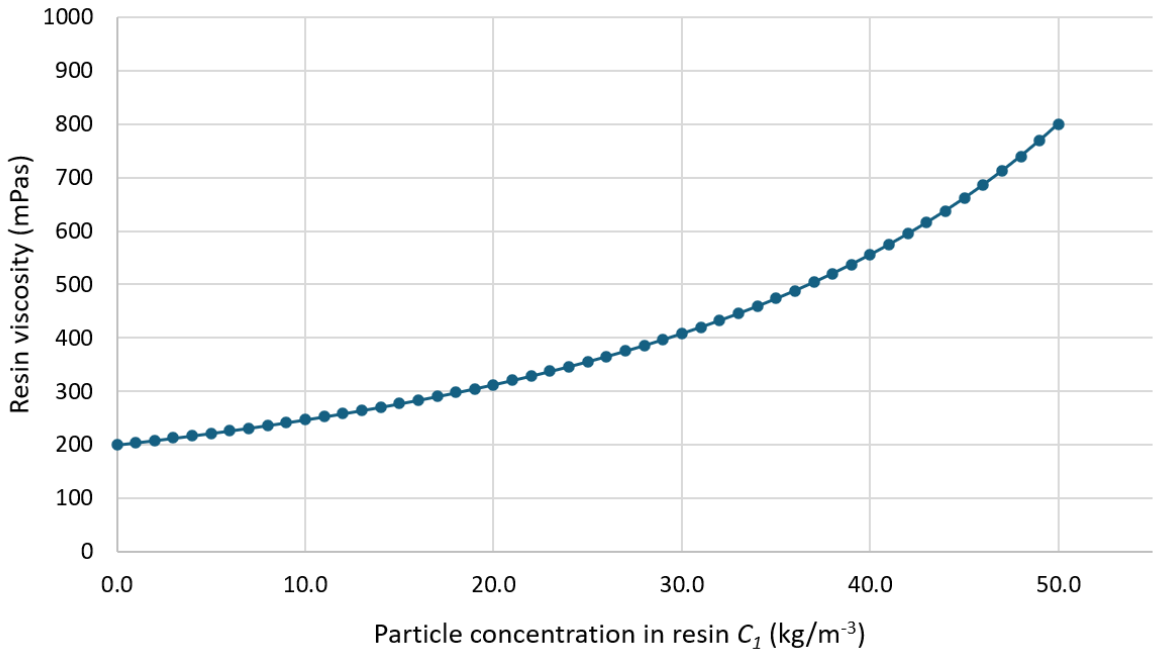

Figure 10: Variation of resin viscosity with particle concentration

2. Methodology

2.7. Particles and Permeability

- The permeability depends on the pore space available for the resin to flow.
- This available space reduces with increasing particle filtration, thereby decreasing the permeability.
- It is assumed that the particle filtration results in a uniform coating over the cylindrical tow surfaces, as shown in Fig. 9.
- The updated permeability can be estimated using the Gebart permeability model (Eq. 7) by modifying the preform volume fraction [14].

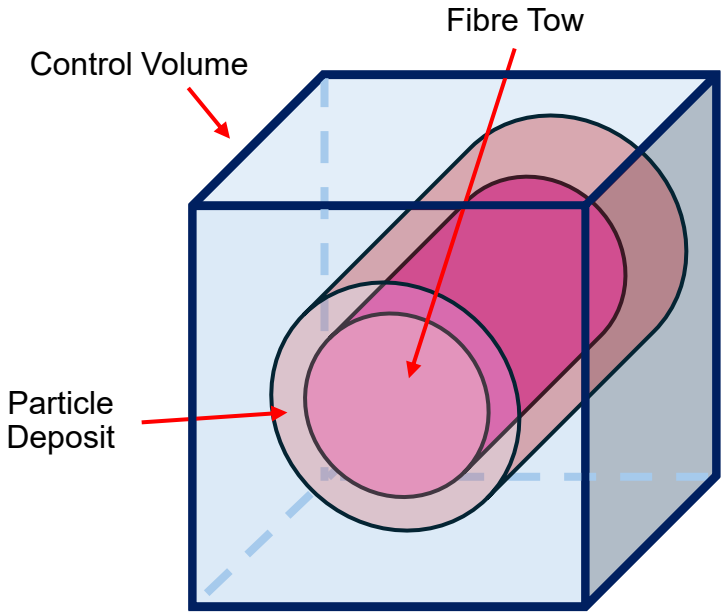

Figure 9: Parameters for permeability update

$$K_{new} = \frac{16}{9\pi\sqrt{2}}\left(\sqrt{\frac{V_{fmax}}{V_f + V_P}} - 1\right)^{5/2} {R_{final}}^2 \qquad (7)$$

V_{fmax} = Maximum volume fraction

V_f = Initial preform volume fraction

V_P = Filtered particle volume fraction = C_2/ρ_P

R_{final} = Final tow radius

2. Methodology

2.8. Transport Model Configuration

Partially Coupled Model

- In this approach, the resin viscosity/ preform permeability is assumed to be constant and unaffected by the presence of particles (Fig. 11a)

- After the pressure and velocity fields are solved, the particle concentrations are updated based on the resin flow, resulting in a passive transport.

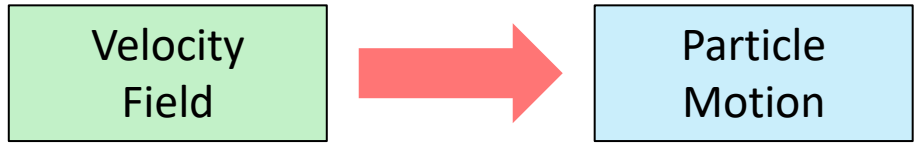

Figure 11a: Partially coupled model

Fully Coupled Model

- In this approach, the resin viscosity/ preform permeability is updated at each time step according to the concentration of particles within an element (Fig. 11b).

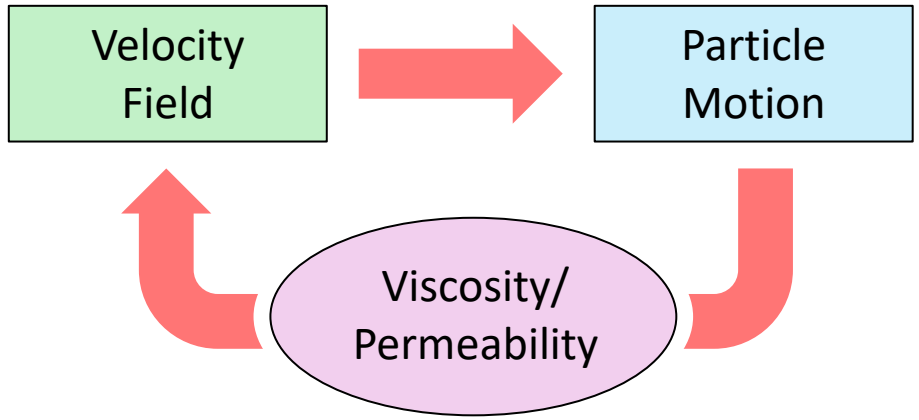

Figure 11b: Fully coupled model

3. Results

3.1. Numerical Flow Domain

- The numerical domain is a $10cm \times 30cm$ rectangular mould, and the resin is injected under controlled pressure/ flow conditions from a line gate, as shown in Fig. 12.

- Particles are introduced to the system from the inlet under different conditions, and the final distribution of particles within the resin and filtered particles is analysed.

- The numerical parameters are given in Table 1.

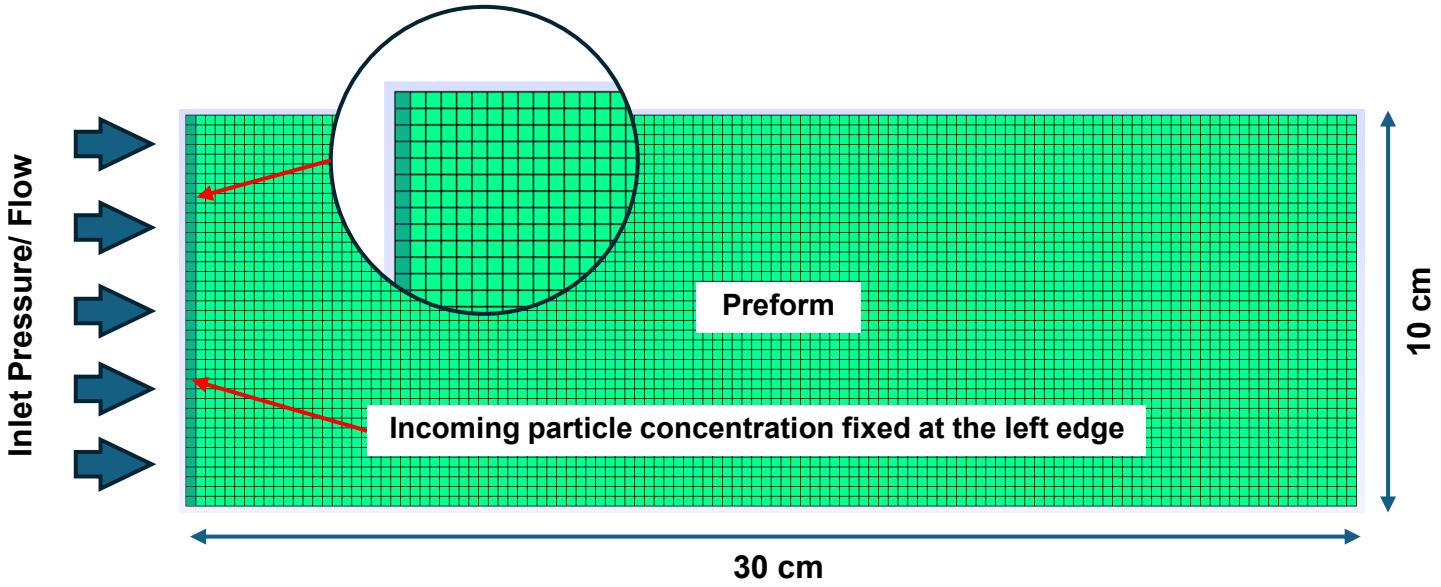

Figure 12: Numerical domain setup

Table 1: Flow simulation parameters

Parameter	Value
Preform permeability	5e-11 m^2
Resin viscosity	200 mPas
Preform volume fraction	0.5
Mould thickness	5 mm

3. Results

3.2. Partially Coupled Model

- Particle transport was simulated under constant inlet flow rate conditions with a fixed inlet concentration of 10 kg/m^3.
- Fig. 13a shows the final distribution of particles within the resin (C_1) and the filtered particles (C_2) with and without filtration effects.
- In this case, the preform permeability and resin viscosity are unaffected by the presence of particles (Figs.13a,b)

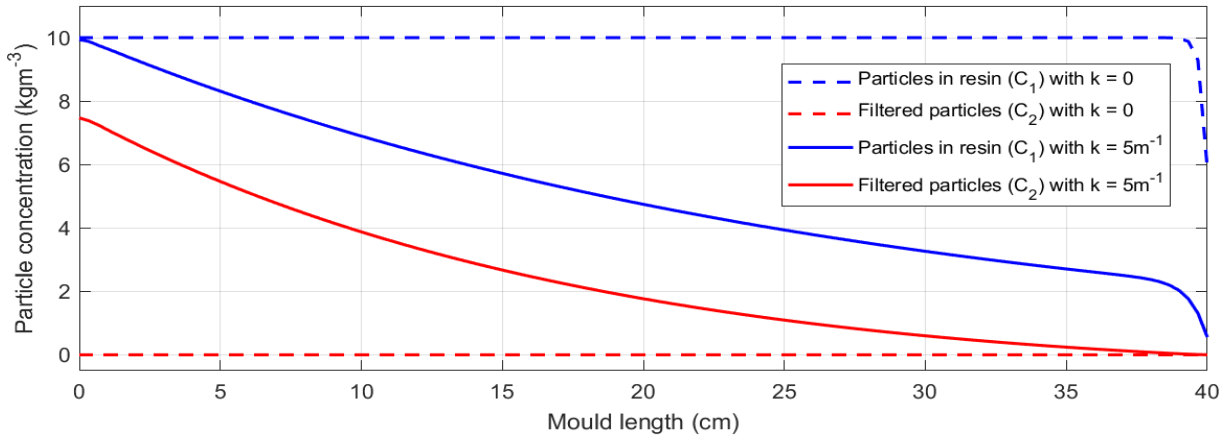

Figure 13a: Distribution of particles at the end of mould filling

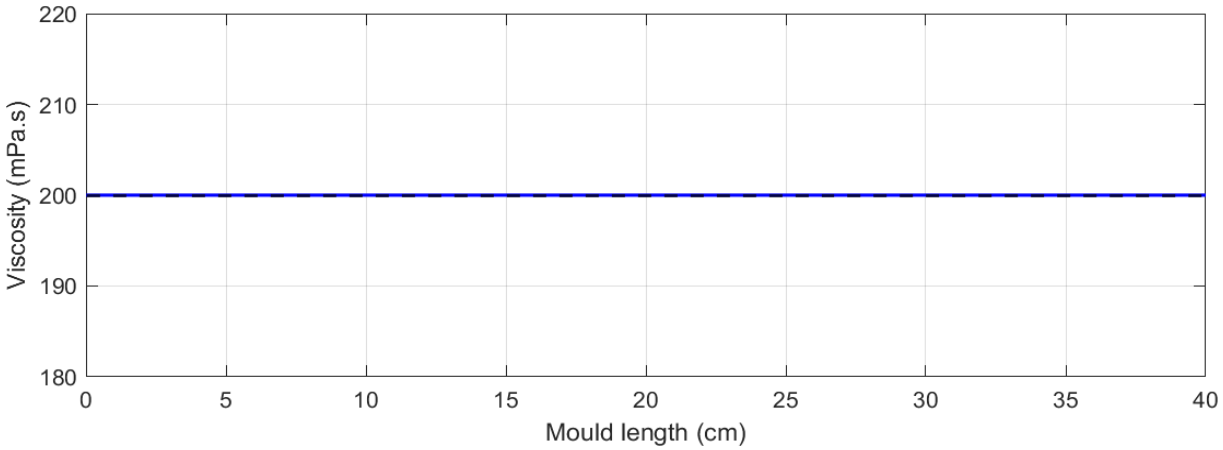

Figure 13b: Variation of the resin viscosity at the end of mould filling

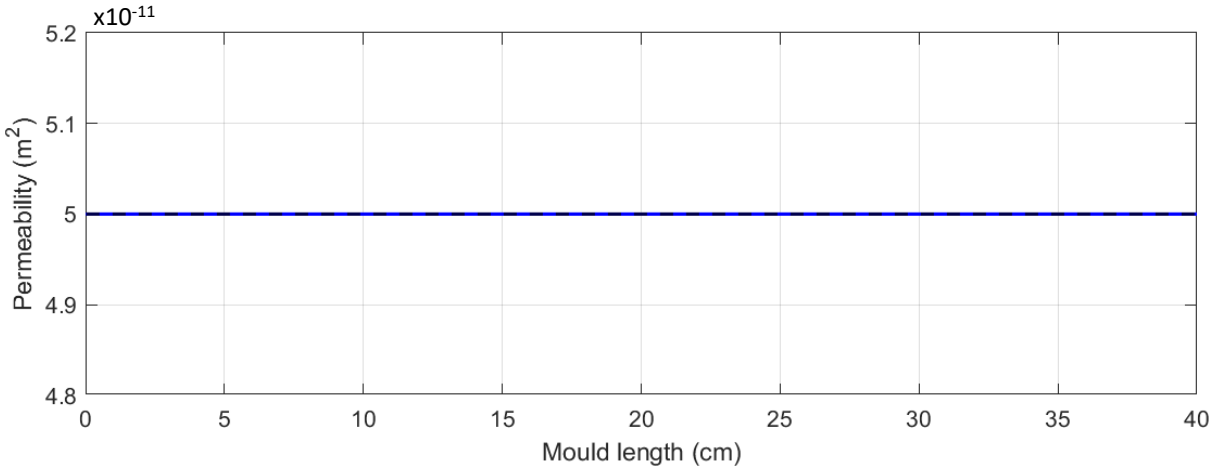

Figure 13c: Variation of the preform permeability at the end of mould filling

3. Results

3.3. Fully Coupled Model

- Here, the resin viscosity and preform permeability become dependent on C_1 and C_2, respectively.
- The initial resin viscosity was $200 mPa.s$, and the initial preform permeability was $5 \times 10^{-11}\, m^2$.
- As shown in Fig. 14, the viscosity and permeability deviate from their initial values in regions with high particle concentrations.

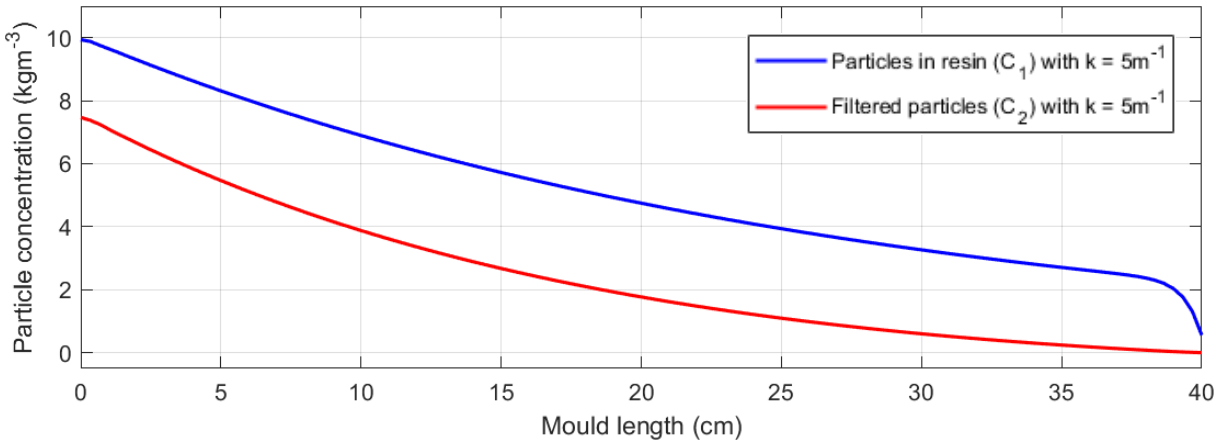

Figure 14a: Distribution of particles ($\boldsymbol{k}$ **= 5 m^{-1}**) at the end of mould filling

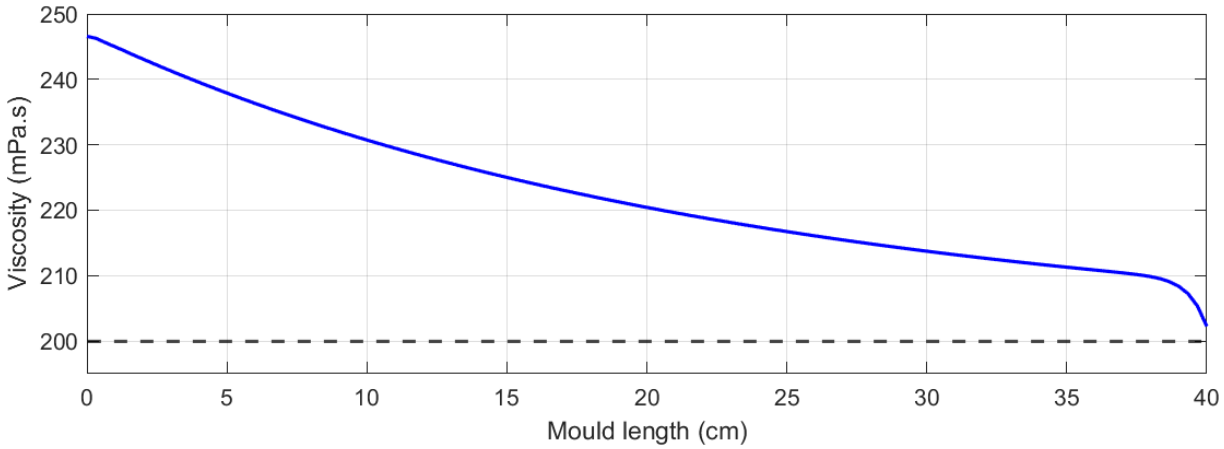

Figure 14b: Variation of the resin viscosity at the end of mould filling

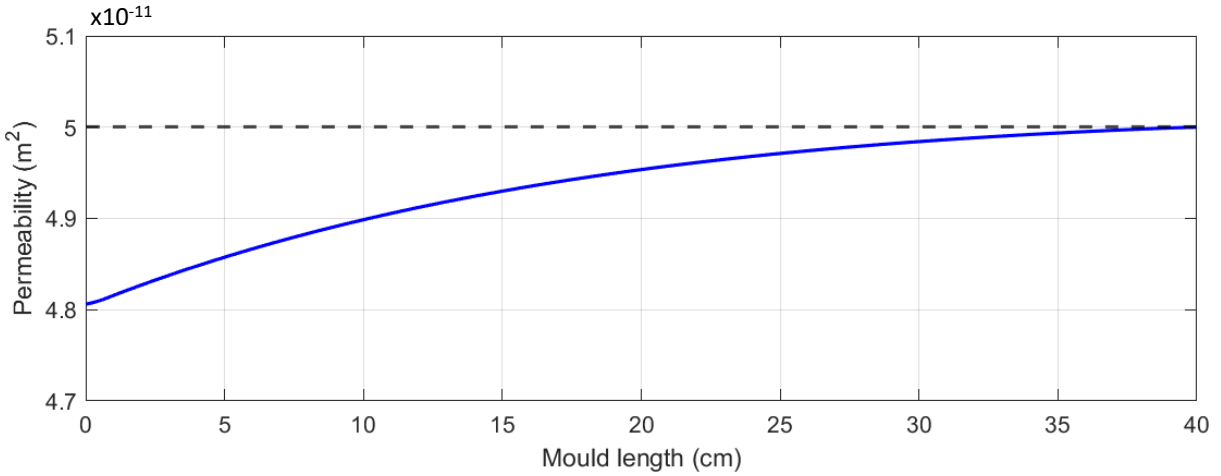

Figure 14c: Variation of the preform permeability at the end of mould filling

3. Results

3.3. Fully Coupled Model

- Here, the resin viscosity and preform permeability become dependent on C_1 and C_2, respectively.
- The initial resin viscosity was $200 mPa.s$, and the initial preform permeability was $5 \times 10^{-11}\, m^2$.
- As shown in Fig. 14, the viscosity and permeability deviate from their initial values in regions with high particle concentrations.

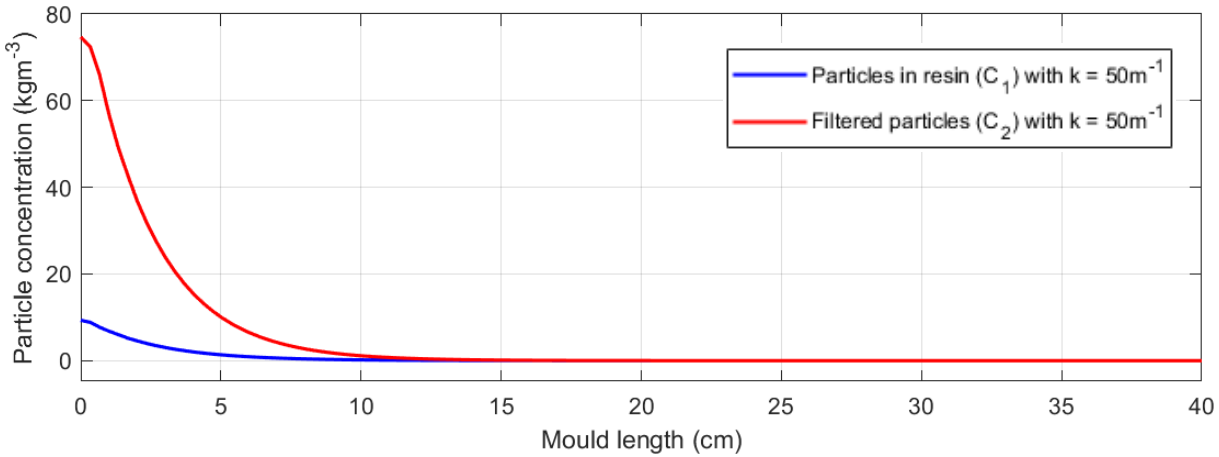

Figure 15a: Distribution of particles ($\boldsymbol{k}$ **= 50 m^{-1}**) at the end of mould filling

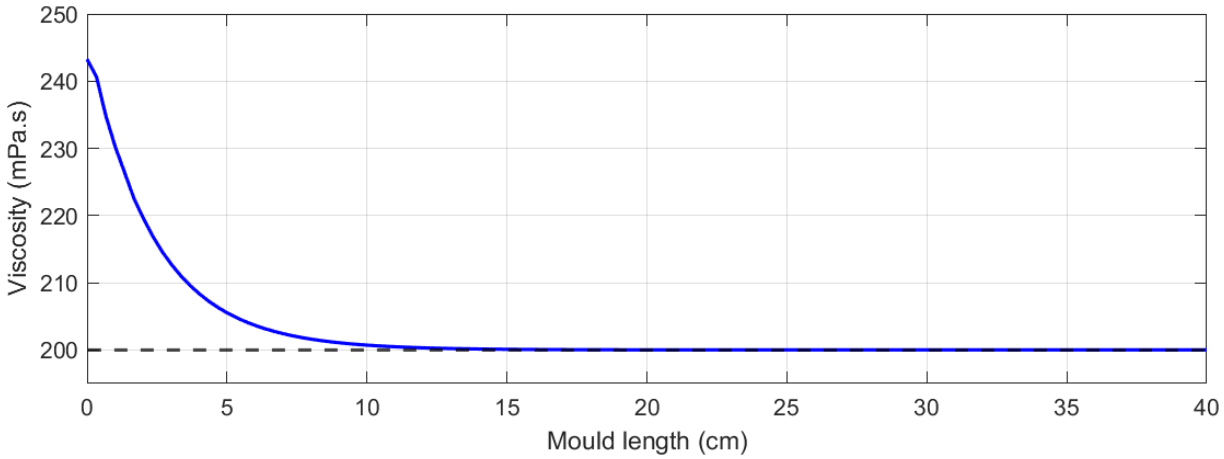

Figure 15b: Variation of the resin viscosity at the end of mould filling

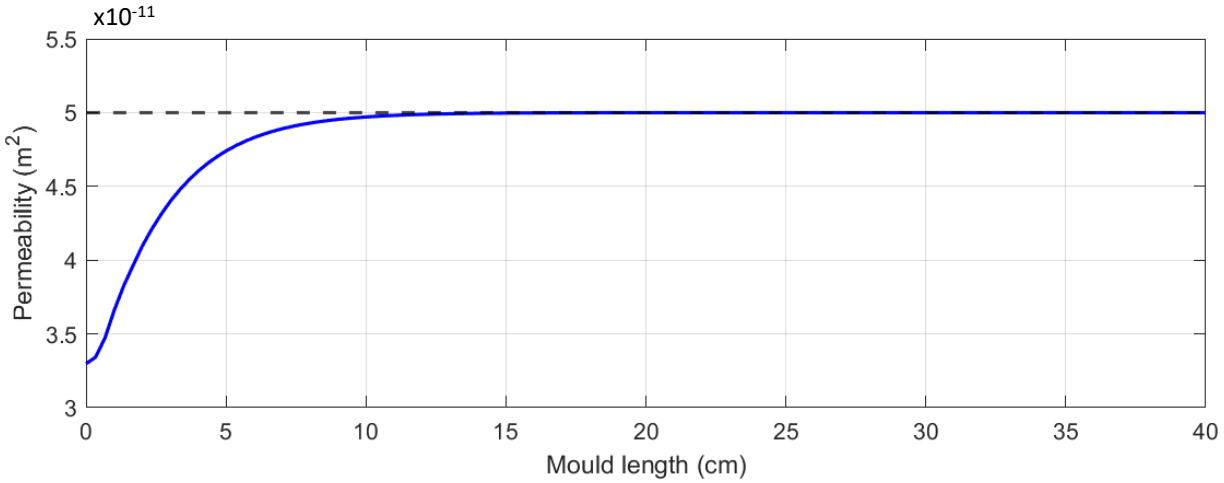

Figure 15c: Variation of the preform permeability at the end of mould filling

3. Results

3.4. Impact of the Particle Presence

- The presence of particles significantly alters the mould fill time and the pressures generated within the mould, compared to an injection of pure resin (Fig. 16).

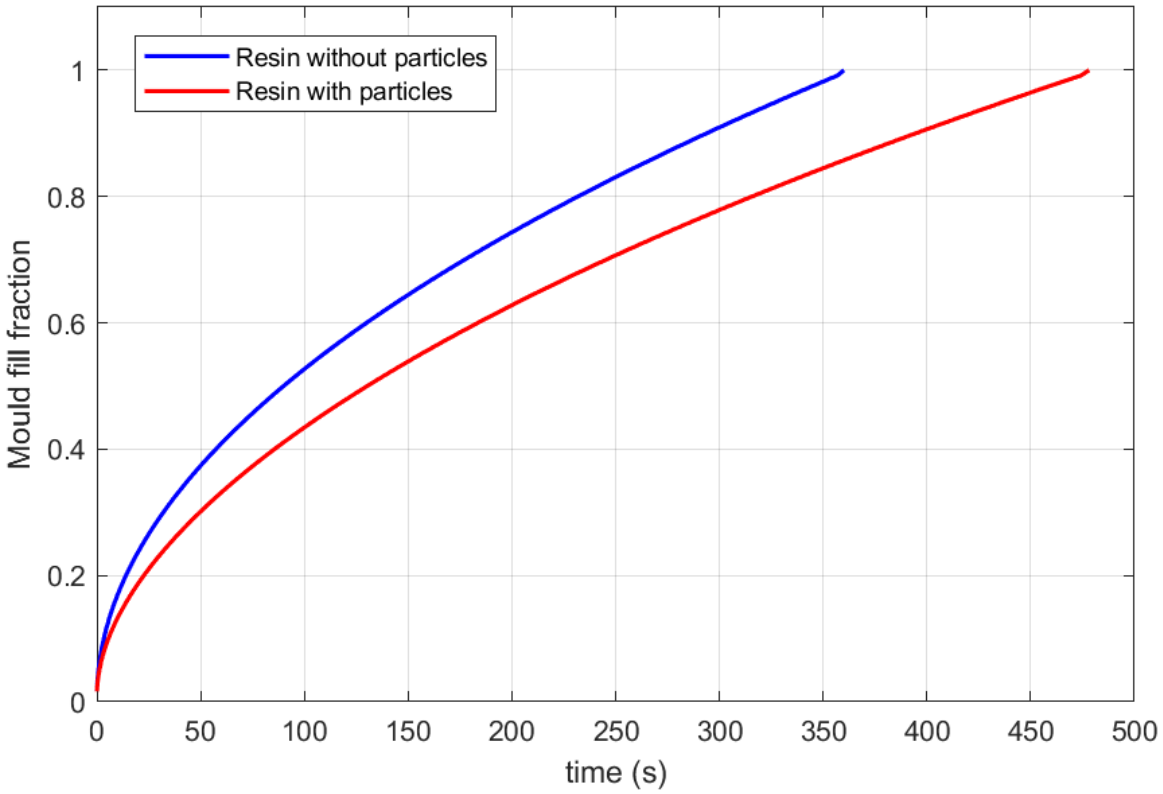

Figure 16a: Variation of mould fill fraction with time for a fixed pressure resin injection

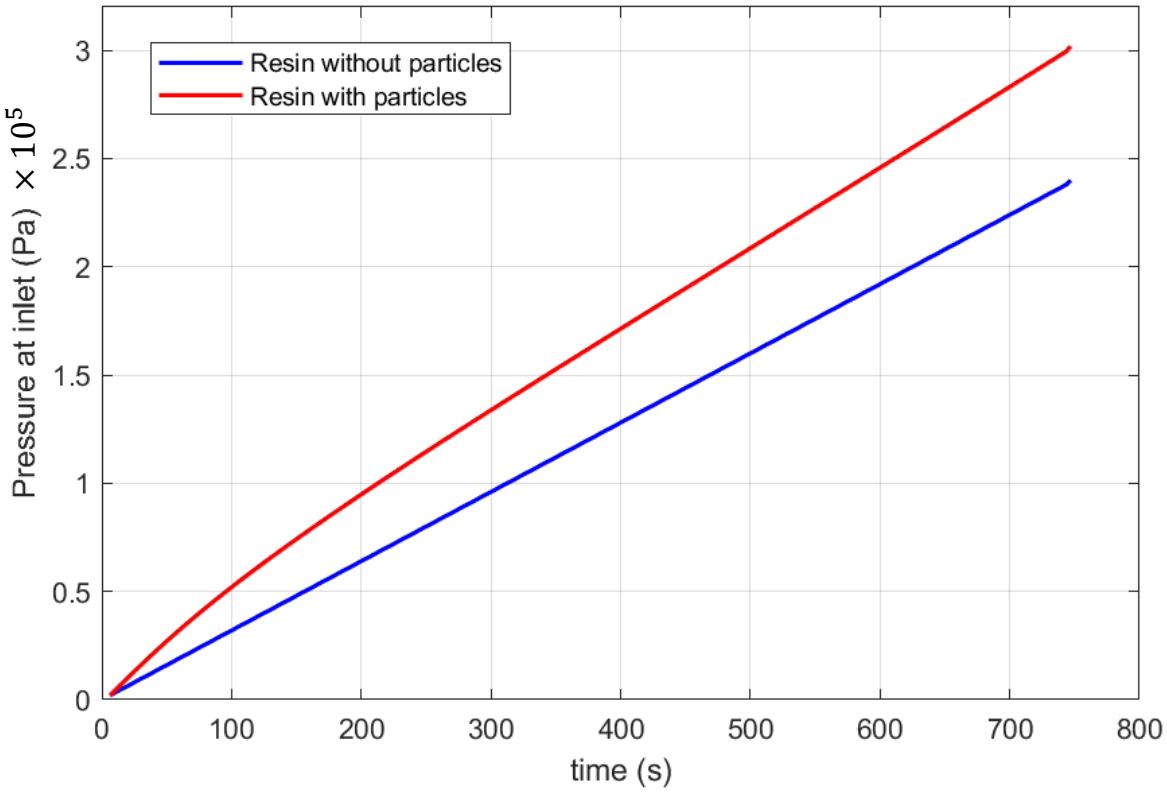

Figure 16b: Variation of pressure at the inlet with time for a fixed flow rate resin injection

3. Results

3.5. Mould Fill Time under Fixed Pressure Injection

- The incoming particle concentration (C_1) and the filtration coefficient (k) were varied while recording the mould fill time.
- It was seen that the mould fill time increased with the increasing C_1 (Fig 17).
- This can be attributed to the resin viscosity increase and permeability decrease caused by the increasing presence of particles within the system.
- It was also seen that for a given C_1 value, there existed a specific value of k at which the mould fill time was minimum (Fig. 17).

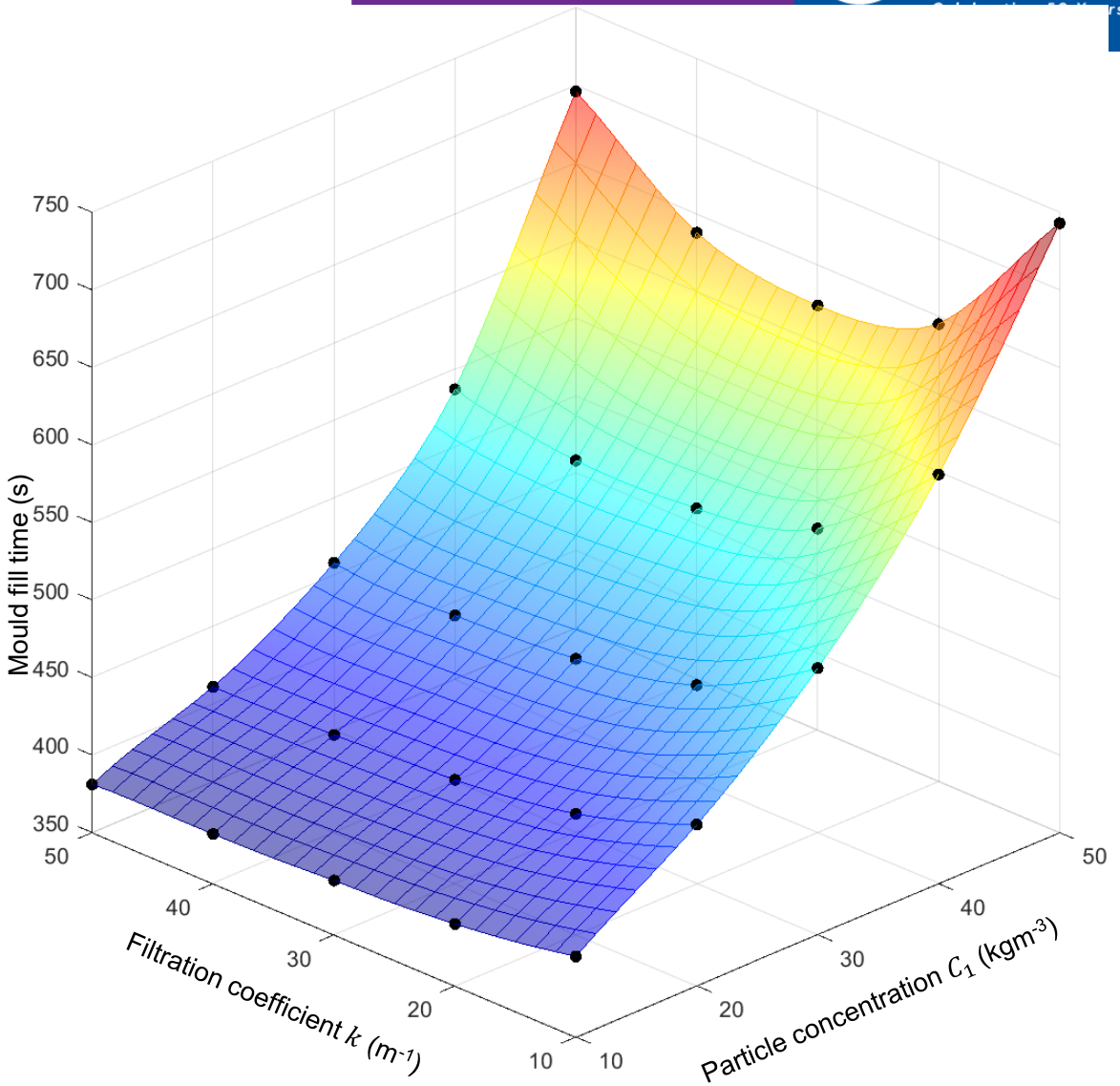

Figure 17: Variation of mould fill time

3. Results

3.6. Pressure at Inlet under Fixed Flowrate Injection

- Here, the incoming particle concentration (C_1) and the filtration coefficient (k) were varied while monitoring the pressure at the resin inlet.
- In a trend similar to the previous case, the pressure at the inlet increased with C_1. (Fig 18)
- Large pressures were observed when both C_1 and k were high.

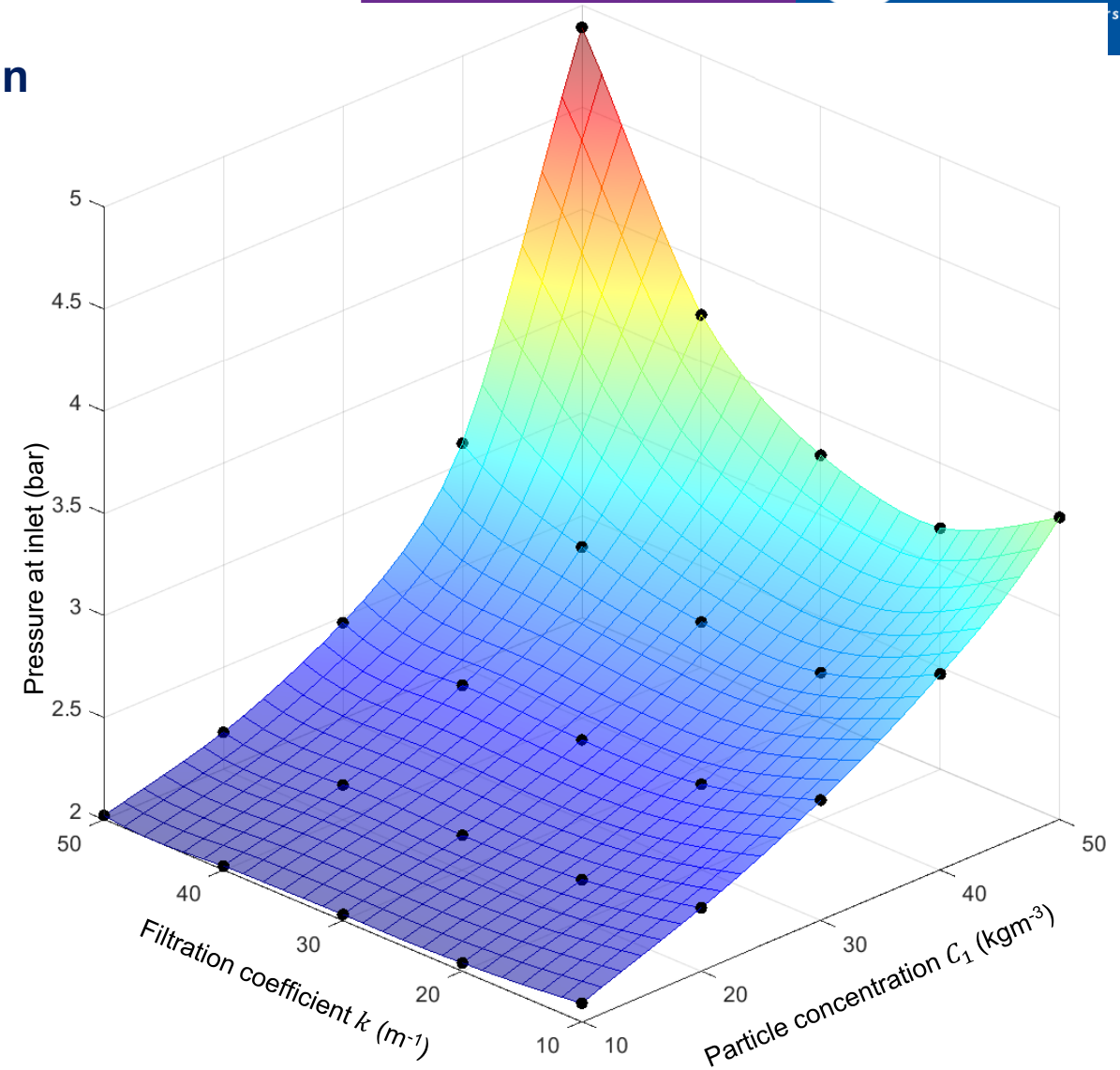

Figure 18: Variation of pressure at the inlet

3. Results

3.7. Influence of Filtration Coefficient

- The influence of the filtration coefficient (k) on the particle distributions (C_1 and C_2) at the end of mould filling was investigated (Figs. 19a and 19b).
- At very low values of k, particle distribution within the fibre preform tends towards homogeneity.
- However, for realistic k values, severe filtration causes the particles to accumulate near the resin inlet.
- This leads to increasingly non-homogeneous particle distributions at the end of mould filling.

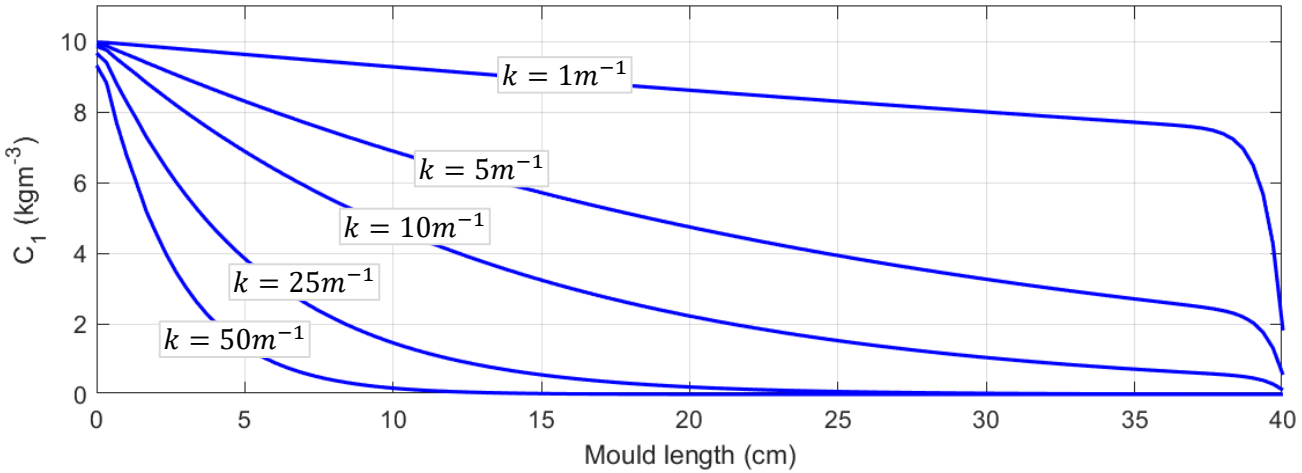

Figure 19a: Variation of C_1 with k

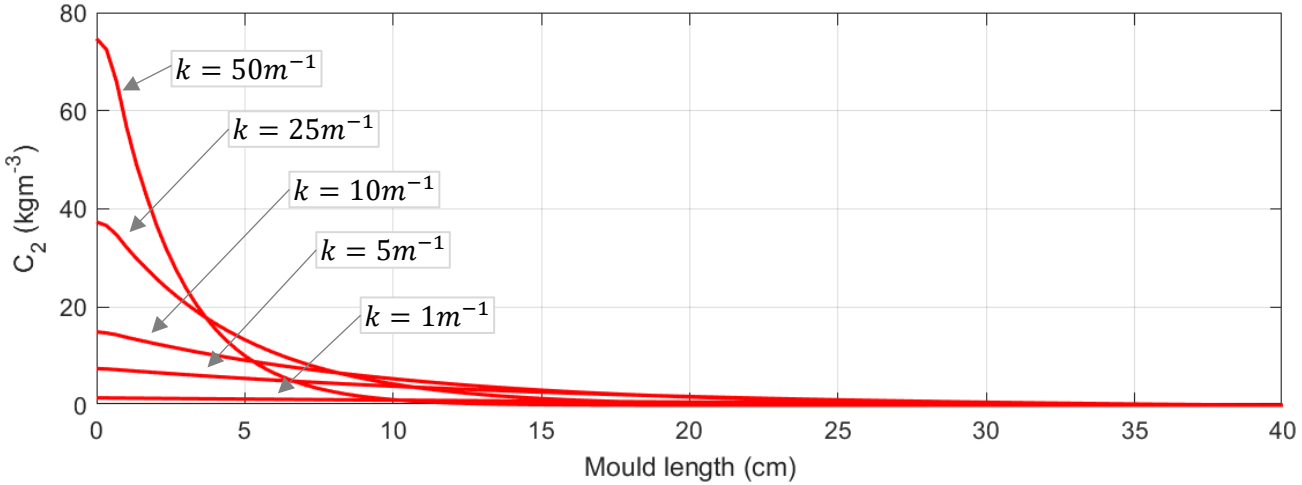

Figure 19b: Variation of C_2 with k

3. Results

3.8. Influence of Racetracking

- Racetracking is an important phenomenon that occurs during RTM mould filling, and has a significant impact on the resin flow front evolution and the mould fill time.

- Racetracking was introduced to the current model by increasing the permeability of elements along the mould edges, as shown on Fig. 20.

- The permeability of the racetrack elements was set to be 100x the permeability of the preform elements.

- The racetrack element permeability was unaltered, due to the absence of particle filtration.

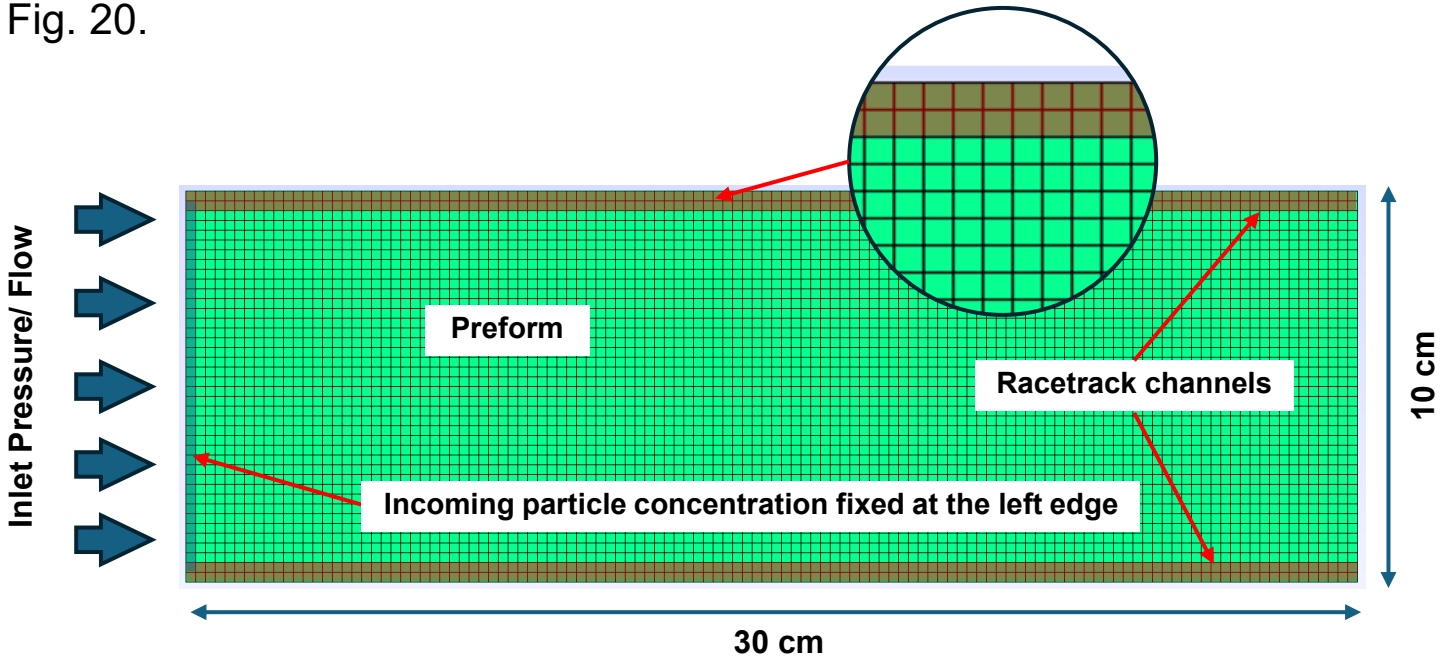

Figure 20: Implementing racetracking along mould edges

3. Results

3.8. Influence of Racetracking

- Racetracking results in a 2-dimensional flow of resin, and strongly influences the final distribution of particles as shown in Fig. 21.

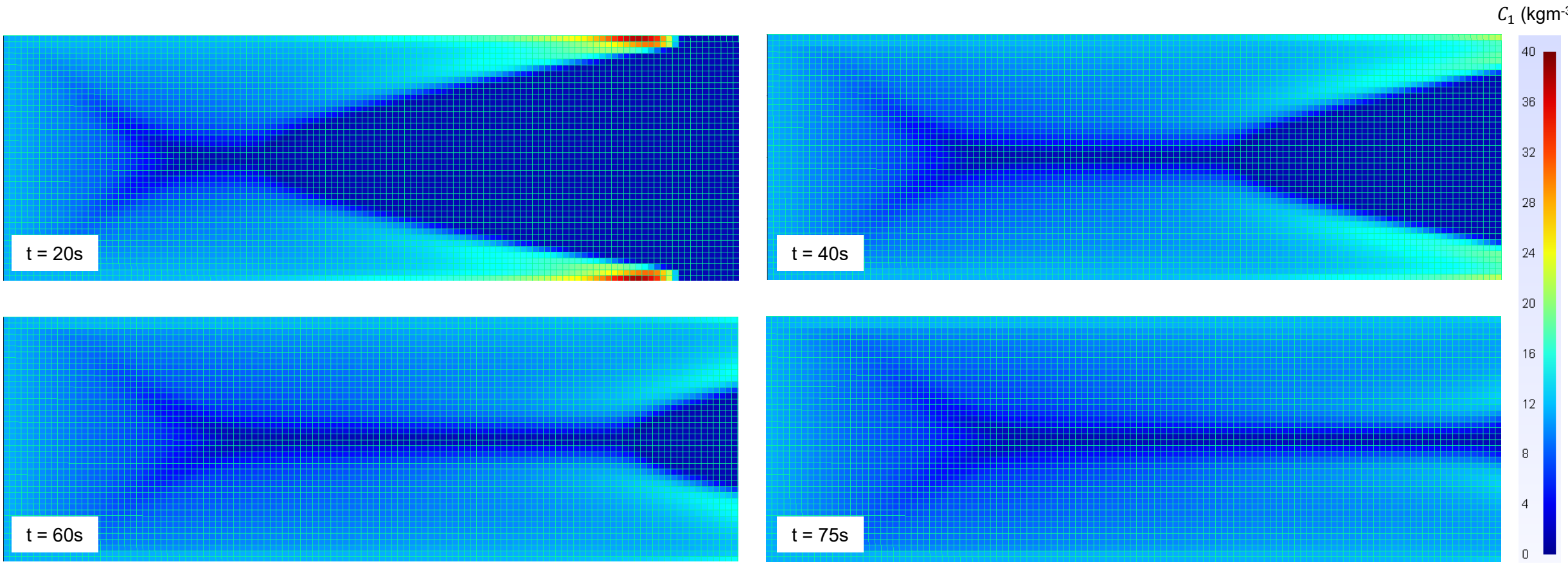

Figure 21: Evolution of particles in resin (C_1) distribution with time during mould filling

3. Results

3.8. Influence of Racetracking

- Racetracking results in a 2-dimensional flow of resin, and strongly influences the final distribution of particles as shown in Fig. 22.

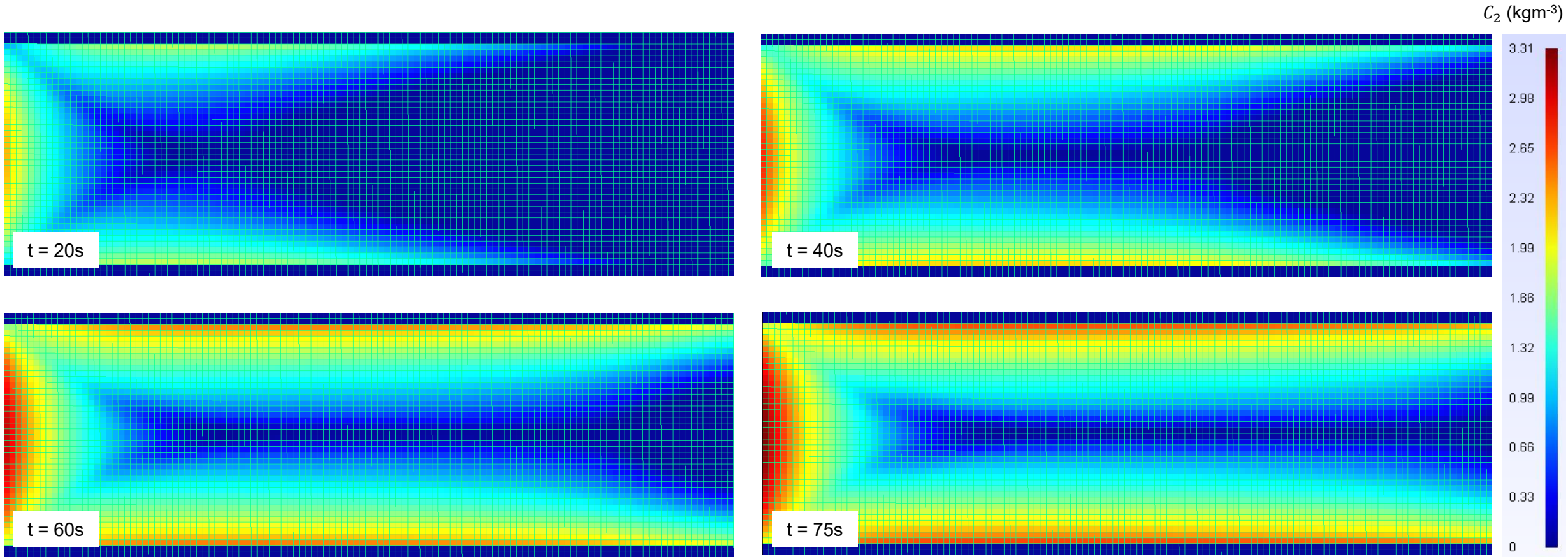

Figure 22: Evolution of filtered particle (C_2) distribution with time during mould filling

3. Results

3.8. Influence of Racetracking

- Racetracking results in a 2D flow of resin, and strongly influences the final distribution of particles as shown in Figs. 18 & 19.
- Since the flow rapidly develops along the mould edges, particles are introduced to the mould extremities.
- Therefore, compared to the 1D case, the distribution of particles within the resin is higher when racetracking (i.e., *high permeability flow paths*) is present.
- This could be an indicator of a potential method of achieving more uniform particle distributions.
- However, this approach also results in the loss of a certain particle mass, which may be a limiting factor.

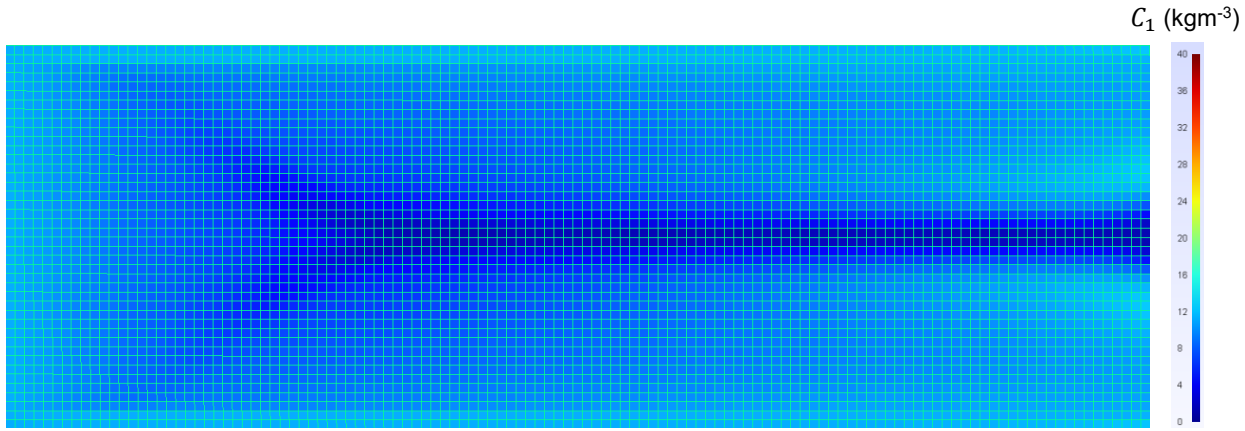

Figure 21: Distribution of particles in resin (C_1) at the end of mould filling

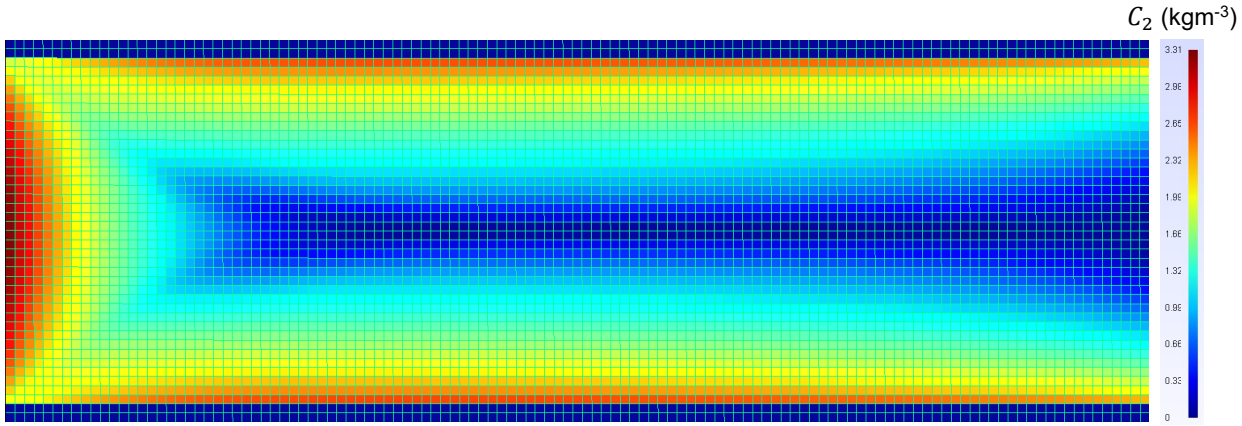

Figure 22: Distribution of filtered particles (C_2) at the end of mould filling

4. Summary and Outlook

- The transport of particle mass concentrations during resin impregnation was modelled and simulated using LIMS and MPI.
- Pressure and velocity fields were solved using LIMS, and these were used by a worker script to transport the particles.
- The updated permeabilities and viscosities computed by the worker were sent back to LIMS, allowing fully coupled simulations.
- The influence of particle presence, resin injection conditions, filtration coefficient, and racetracking was investigated.
- It was found that the combination of incoming particle concentration and the filtration coefficient has a strong influence on the particle distribution at the end of mould filling.
- 2D flows resulting from high permeability flow channels (such as racetracking) show potential over 1D flows to obtain more uniform particle dispersion.
- In line with this, the influence of high permeability channels and multipoint resin injections on dispersion uniformity needs to be evaluated.

References

[1] R. Shanthar, R. Prosser, P. Potluri, C. Abeykoon, and S. G. Advani, 'Modelling and simulation of the polymer resin flow through fibres during Resin Transfer Moulding: a comprehensive review', Compos. Part Appl. Sci. Manuf., vol. 208, p. 109839, Sep. 2026, doi: 10.1016/j.compositesa.2026.109839.

[2] J. Barroeta Robles et al., 'Processing and properties of graphene-enhanced glass fibre composites using a scalable manufacturing process', Compos. Struct., vol. 267, p. 113874, Jul. 2021, doi: 10.1016/j.compstruct.2021.113874.

[3] B. M. Louis, J. Maldonado, F. Klunker, and P. Ermanni, 'Particle distribution from in-plane resin flow in a resin transfer molding process', Polym. Eng. Sci., vol. 59, no. 1, pp. 22–34, 2019, doi: 10.1002/pen.24860.

[4] M. Chohra, S. G. Advani, A. Gokce, and S. Yarlagadda, 'Modeling of filtration through multiple layers of dual scale fibrous porous media', Polym. Compos., vol. 27, no. 5, pp. 570–581, 2006, doi: 10.1002/pc.20228.

[5] W. R. Hwang, S. G. Advani, and S. Walsh, 'Direct simulations of particle deposition and filtration in dual-scale porous media', Compos. Part Appl. Sci. Manuf., vol. 42, no. 10, pp. 1344–1352, 2011.

[6] Y. Djebara, A. Imad, A. Saouab, and T. Kanit, 'A numerical modelling for resin transfer molding (RTM) process and effective thermal conductivity prediction of a particle–filled composite carbon–epoxy', J. Compos. Mater., vol. 55, no. 1, pp. 3–15, Jan. 2021, doi: 10.1177/0021998320940035.

[7] M. Erdal, S. I. Güçeri, and S. C. Danforth, 'Impregnation Molding of Particle-Filled Preceramic Polymers: Process Modeling', J. Am. Ceram. Soc., vol. 82, no. 8, pp. 2017–2028, 1999, doi: 10.1111/j.1151-2916.1999.tb02034.x.

[8] D. Abliz, D. C. Berg, and G. Ziegmann, 'Flow of quasi-spherical nanoparticles in liquid composite molding processes. Part II: Modeling and simulation', Compos. Part Appl. Sci. Manuf., vol. 125, p. 105562, Oct. 2019, doi: 10.1016/j.compositesa.2019.105562.

[9] D. Lefevre, S. Comas-Cardona, C. Binétruy, and P. Krawczak, 'Modelling the flow of particle-filled resin through a fibrous preform in liquid composite molding technologies', Compos. Part Appl. Sci. Manuf., vol. 38, no. 10, pp. 2154–2163, Oct. 2007, doi: 10.1016/j.compositesa.2007.06.008.

[10] D. Lefevre, S. Comas-Cardona, C. Binetruy, and P. Krawczak, 'Coupling filtration and flow during liquid composite molding: Experimental investigation and simulation', Compos. Sci. Technol., vol. 69, no. 13, pp. 2127–2134, Oct. 2009, doi: 10.1016/j.compscitech.2009.05.008.

[11] M. Nordlund, S. P. Fernberg, and T. S. Lundström, 'Particle deposition mechanisms during processing of advanced composite materials', Compos. Part Appl. Sci. Manuf., vol. 38, no. 10, pp. 2182–2193, Oct. 2007, doi: 10.1016/j.compositesa.2007.06.009.

[12] P. Simacek, N. Niknafs Kermani, and S. G. Advani, 'Coupled Process Modeling of Flow and Transport Phenomena in LCM Processing', Integrating Mater. Manuf. Innov., vol. 11, no. 3, pp. 363–381, Sep. 2022, doi: 10.1007/s40192-022-00268-1.

[13] R. Deepak Selvakumar and S. Dhinakaran, 'Effective viscosity of nanofluids — A modified Krieger–Dougherty model based on particle size distribution (PSD) analysis', J. Mol. Liq., vol. 225, pp. 20–27, Jan. 2017, doi: 10.1016/j.molliq.2016.10.137.

[14] B. R. Gebart, 'Permeability of Unidirectional Reinforcements for RTM', J. Compos. Mater., vol. 26, no. 8, pp. 1100–1133, Aug. 1992, doi: 10.1177/002199839202600802.

References

[1] R. Shanthar, R. Prosser, P. Potluri, C. Abeykoon, and S. G. Advani, '**Modelling and simulation of the polymer resin flow through fibres during Resin Transfer Moulding: a comprehensive review**', Compos. Part Appl. Sci. Manuf., vol. 208, p. 109839, Sep. 2026, doi: 10.1016/j.compositesa.2026.109839.

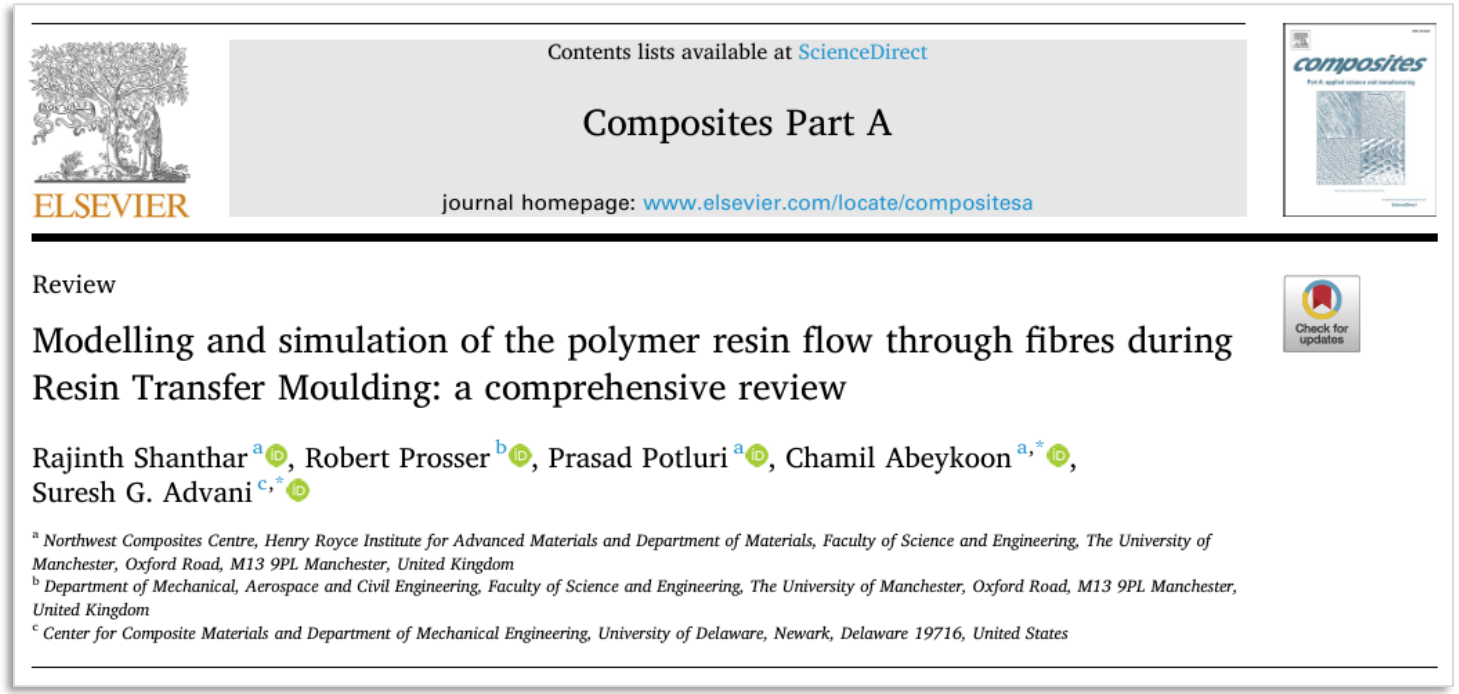

Contents lists available at ScienceDirect

Composites Part A

journal homepage: www.elsevier.com/locate/compositesa

Review

Modelling and simulation of the polymer resin flow through fibres during Resin Transfer Moulding: a comprehensive review

Rajinth Shanthar [a], Robert Prosser [b], Prasad Potluri [a], Chamil Abeykoon [a,*], Suresh G. Advani [c,*]

[a] Northwest Composites Centre, Henry Royce Institute for Advanced Materials and Department of Materials, Faculty of Science and Engineering, The University of Manchester, Oxford Road, M13 9PL Manchester, United Kingdom
[b] Department of Mechanical, Aerospace and Civil Engineering, Faculty of Science and Engineering, The University of Manchester, Oxford Road, M13 9PL Manchester, United Kingdom
[c] Center for Composite Materials and Department of Mechanical Engineering, University of Delaware, Newark, Delaware 19716, United States

Thank You

Q&A